JVI Journals.ASM.org

Primary Human Macrophages Serve as Vehicles for Vaccinia Virus Replication and Dissemination

Daniel Byrd,[a] Nicole Shepherd,[a] Jie Lan,[a] Ningjie Hu,[b] Tohti Amet,[a] Kai Yang,[a,b] Mona Desai,[c] Qigui Yu[a,c]

Department of Microbiology and Immunology and Center for AIDS Research, Indiana University School of Medicine, Indianapolis, Indiana, USA[a]; Zhejiang Provincial Key Laboratory for Technology & Application of Model Organisms, Wenzhou Medical College, University Park, Wenzhou, China[b]; Division of Infectious Diseases, Department of Medicine, Indiana University School of Medicine, Indianapolis, Indiana, USA[c]

ABSTRACT

Human monocytic and professional antigen-presenting cells have been reported only to exhibit abortive infections with vaccinia virus (VACV). We found that monocyte-derived macrophages (MDMs), including granulocyte macrophage colony-stimulating factor (GM-CSF)-polarized M1 and macrophage colony-stimulating factor (M-CSF)-polarized M2, but not human AB serum-derived cells, were permissive to VACV replication. The titers of infectious virions in both cell-free supernatants and cellular lysates of infected M1 and M2 markedly increased in a time-dependent manner. The majority of virions produced in permissive MDMs were extracellular enveloped virions (EEV), a secreted form of VACV associated with long-range virus dissemination, and were mainly found in the culture supernatant. Infected MDMs formed VACV factories, actin tails, virion-associated branching structures, and cell linkages, indicating that MDMs are able to initiate *de novo* synthesis of viral DNA and promote virus release. VACV replication was sensitive to inhibitors against the Akt and Erk1/2 pathways that can be activated by VACV infection and M-CSF stimulation. Classical activation of MDMs by lipopolysaccharide (LPS) plus gamma interferon (IFN-γ) stimulation caused no effect on VACV replication, while alternative activation of MDMs by interleukin-10 (IL-10) or LPS-plus-IL-1β treatment significantly decreased VACV production. The IL-10-mediated suppression of VACV replication was largely due to Stat3 activation, as a Stat3 inhibitor restored virus production to levels observed without IL-10 stimulation. In conclusion, our data demonstrate that primary human macrophages are permissive to VACV replication. After infection, these cells produce EEV for long-range dissemination and also form structures associated with virions which may contribute to cell-cell spread.

IMPORTANCE

Our results provide critical information to the burgeoning fields of cancer-killing (oncolytic) virus therapy with vaccinia virus (VACV). One type of macrophage (M2) is considered a common presence in tumors and is associated with poor prognosis. Our results demonstrate a preference for VACV replication in M2 macrophages and could assist in designing treatments and engineering poxviruses with special considerations for their effect on M2 macrophage-containing tumors. Additionally, this work highlights the importance of macrophages in the field of vaccine development using poxviruses as vectors. The understanding of the dynamics of poxvirus-infected foci is central in understanding the effectiveness of the immune response to poxvirus-mediated vaccine vectors. Monocytic cells have been found to be an important part of VACV skin lesions in mice in controlling the infection as well as mediating virus transport out of infected foci.

Orthopoxvirus, a genus of the subfamily *Chordopoxvirinae* of the family *Poxviridae*, is composed of large DNA viruses that infect a wide array of mammalian species. The most famous member of the genus is the human-specific variola virus, which causes smallpox. In nature, variola virus has a strict human-specific tropism, and nonhuman reservoirs of the virus have never been found. Variola virus is generally transmitted via inhalation, with subsequent infection and replication in epithelial cells of the oral and respiratory mucosa. The next stage of infection involves viral infiltration of lymphoid organs accompanied by strong viremia and skin lesions. Recent studies using high doses of variola virus to infect *Cynomolgus macaques* in an attempt to develop an animal model of smallpox have demonstrated that infected animals develop systemic infection and hemorrhagic symptoms (1, 2). These symptoms were correlated with monocyte/macrophage-mediated viremia and dissemination (1, 2). In mice, macrophages are crucial to control the infection of the orthopoxvirus ectromelia virus (ECTV) (3, 4). However, ECTV replicates in macrophages (5) and directly contributes to dissemination within the host (6). Given their importance in defense against invading pathogens, macrophages likely act as a double-edged sword in certain orthopoxvirus infections, mediating both infection control and virus dissemination.

The relatively benign vaccinia virus (VACV), the prototypical member of the orthopoxvirus genus, has a genome 95% homologous to variola virus (7) and is most often used as a model of orthopoxvirus infection. With its high antigenic homology, VACV has been crucial as a live vaccine for the global eradication of smallpox throughout the 20th century. VACV produces four virion forms, including the single-enveloped intracellular mature virion (IMV), triple-enveloped intracellular enveloped virion

Received 15 December 2013 **Accepted** 27 March 2014
Published ahead of print 2 April 2014
Editor: K. Frueh
Address correspondence to Qigui Yu, andyu@iupui.edu.

doi:10.1128/JVI.03726-13

(IEV), the double enveloped, cell-associated enveloped virion (CEV), and extracellular enveloped virion (EEV) (8). Similar to variola virus but without the severe effects, VACV can produce a generalized infection which involves EEV viremia with subsequent infection of distant sites on the skin (8). Additionally, CEV can rapidly transfer between neighboring cells in culture via actin tails (9), although the precise routes of long-range dissemination via viremia are unknown. Visualizations of VACV skin lesions in mice have shown that highly motile infected macrophages are adjacent to infected skin foci (10). Extraction and analysis of these macrophages have revealed that the cells are permissively infected and are associated with 7% of the total VACV in the lesion (10). Thus, macrophages have been exhibited in mammals as potential candidates for mediating long-range VACV dissemination. One report has demonstrated that the infection of primary human macrophages is abortive (11). This study demonstrated that cells only support early stages of the VACV infection cycle, including morphological cytopathic effects, deactivation of host protein synthesis, and activation of early viral protein synthesis, but not late infection stages, including synthesis of late viral proteins, replication of viral DNA, and production of infectious progeny virions (11). VACV infection of primary human monocytes and dendritic cells (DCs) has also been demonstrated to be abortive *in vivo* and *in vitro* (12–18), where viral DNA is only weakly replicated, no late genes are transcribed, and no actin tails or viral factories form. Hence, it has been speculated that, in humans, VACV cannot replicate in monocytic cells, including monocytes, macrophages, and DCs.

Macrophages are found in tissues throughout the body in most organs. These tissue macrophages are mainly derived from circulating monocytes but are difficult to collect and study. To obtain macrophages, researchers have developed several approaches to differentiate primary blood monocytes by incubating them with (i) media containing human AB serum or fetal bovine serum (FBS) (19), (ii) media containing FBS supplemented with granulocyte-macrophage colony-stimulating factor (GM-CSF) or M-CSF (20, 21), or (iii) conditional serum-free media with or without GM-CSF or M-CSF (22, 23). These different methods of MDM generation have not been systematically related to each other functionally or transcriptionally. GM-CSF-induced MDMs replicate some of the functions and transcriptional profiles of classically activated proinflammatory (M1) cells *in vivo*, while M-CSF-induced MDMs tend to replicate alternatively activated anti-inflammatory (M2) macrophages (24). Gene expression profiling studies of murine M2 cells have found some common expression of genes between M2 cells generated *in vitro* and M2 cells from *in vivo* disease models (25, 26). *In vitro* M1 and M2 macrophages largely mirror the functional phenotypes of macrophages *in vivo* for allergy, parasitic infections, and certain cancers (27), but other pathological conditions, such as neurodegenerative diseases, express unique macrophage phenotypes. In contrast, human AB serum-derived MDMs have not been related to particular states *in vivo* so far. In the study reported here, we found that both M1- and M2-polarized macrophages were permissive for VACV infection and replication, whereas human AB serum-derived MDMs could be infected but were abortive, as reported previously (11). Infected M1 and M2 MDMs mainly produced EEV and exhibited virion-associated structures that may promote virus spread to neighboring cells. VACV replication was found to be dependent on known poxvirus-associated signaling pathways, and the activation of Stat3 was strongly inhibitory to virus production.

MATERIALS AND METHODS

Ethics statement. Whole-blood samples or leukapheresis products were obtained from healthy blood donors with written consent obtained from each participant. Investigational protocols were approved by Institutional Review Boards for Human Research at the Indiana University School of Medicine (Indianapolis, IN).

Preparation of primary human monocyte-derived macrophages. To isolate peripheral blood mononuclear cells (PBMCs), whole blood or leukapheresis products obtained from healthy blood donors were separated by Ficoll-Hypaque (Amersham Pharmacia Biotech AB, Uppsala, Sweden) gradients. PBMCs were subjected to monocyte isolation using the monocyte negative isolation kit (Dynal, Oslo, Norway). Monocyte purity was determined to be >95% by CD14 staining and fluorescence-activated cell sorting (FACS). To differentiate cells into macrophages, isolated monocytes were cultured in complete RPMI 1640 medium (RPMI 1640 medium supplemented with 10% fetal bovine serum [FBS], 2 mM L-glutamine, 100 U/ml penicillin, and 100 U/ml streptomycin) supplemented with either 50 ng/ml of recombinant human GM-CSF (rhGM-CSF), 50 ng/ml of rhM-CSF, or RPMI 1640 containing 10% human AB serum (Gemini Bio Products, West Sacramento, CA). Culture media were changed every 3 days. Macrophages were considered fully differentiated by 7 days of culture as determined by morphology. Resting T cells were isolated from the PBMCs using a Pan T cell isolation kit II (Miltenyi Biotec, Auburn, CA), which yielded >95% purity of $CD3^+$ T cells. $CD3^+$ T cells were activated by incubating with anti-CD3/anti-CD28 antibody (Ab)-coated magnetic beads (Life Technologies, Carlsbad, CA) and allowed to culture in complete RPMI 1640 medium for 72 h before use in experiments.

Cytokines, antibodies, and flow-cytometric analysis. The following recombinant human xeno-free cytokines for cell culture were purchased from EMD Millipore (Darmstadt, Germany): recombinant human interleukin-1β (rhIL-1β), rhIL-10, and recombinant human gamma interferon (rhIFN-γ). rhM-CSF and rhGM-CSF (carrier-free) were purchased from BioLegend (San Diego, CA). Ultrapure lipopolysaccharide (LPS) derived from *Salmonella enterica* serotype Minnesota R595 was purchased from InvivoGen (San Diego, CA). The following mouse anti-human monoclonal antibodies (MAbs) conjugated with fluorochromes were purchased from BioLegend (San Diego, CA): anti-CD68 conjugated with Alexa Fluor 488, anti-CD163 conjugated with phycoerythrin (PE), and anti-CD86 conjugated with allophycocyanin. For intracellular staining (ICS) of Stat3 activation or caspase-3, cells were fixed with 2% paraformaldehyde (PFA), permeabilized with 0.1% saponin, and stained with mouse anti-human Stat3 phospho-Tyr705 conjugated with Alexa Fluor 647 or rabbit anti-human caspase-3 (active form) conjugated with fluorescein isothiocyanate (FITC) (BD Biosciences, San Jose, CA). Staining for apoptosis and necrosis with annexin V-FITC plus propidium iodide (PI) was performed using the annexin-V-FLUOS staining kit (Roche, Mannheim, Germany) according to the manufacturer's instructions. FACS was performed using a BD FACSCalibur (BD Biosciences, San Diego, CA), and data were analyzed using FlowJo software (TreeStar, San Carlos, CA). For control staining, appropriate fluorochrome-conjugated isotype-matched controls purchased from BD Biosciences (San Jose, CA) were used in tandem with test Abs.

VACV purification, titration, and infection protocols. The primary VACV strain used in this study was Western Reserve (WR). The enhanced green fluorescent protein (EGFP) reporter virus, VV-EGFP, is a WR strain containing a chimeric gene and includes the influenza virus nucleoprotein, the ovalbumin SIINFEKL peptide, and EGFP that localizes to the nucleus (28). Both VACV WR and VV-EGFP were obtained from J. W. Yewdell (NIH, Bethesda, MD). vA5L-YFP is a recombinant WR VACV constructed with the viral core protein A5L fused to yellow fluorescence protein (YFP), which is suitable for visualizing individual virions (29).

This virus was obtained from B. Moss (NIH, Bethesda, MD). Viral stocks were generated and titrated in chicken embryo fibroblasts (Charles River Laboratories, Wilmington, MA) or the monkey kidney cell line CV-1 (ATCC, Manassas, VA) in complete RPMI 1640 medium. After 3 days of infection, cells were lysed in a Dounce homogenizer. Culture supernatants and cell lysates were then subjected to ultracentrifugation at 25,000 × *g* for 80 min through a 36% sucrose cushion. Pellets were resuspended and subjected to virus purification by ultracentrifugation through a 24 to 40% sucrose gradient as previously described (30). Viral titers were determined by a virus plaque assay. Briefly, CV-1 cells were grown in 6-well plates to 90% confluence and overlaid with various dilutions of purified virus. After 1 h of incubation, cells were washed and overlaid with complete RPMI 1640 containing 1.5% carboxylmethylcellulose to prevent *de novo* EEV plaque formation. After 2 to 3 days of culture, cells were stained with a 0.01% crystal violet and 15% ethanol solution and then washed so that plaques could be counted to calculate virus PFU.

For all experiments involving VACV infection of primary MDMs, cells were first plated in 12- or 6-well plates with 50,000 to 300,000 cells per well, incubated with VACV WR at a multiplicity of infection (MOI) of 5 for 1 h, washed three times with phosphate-buffered saline (PBS), and allowed to culture for 2 days in complete RPMI 1640. Culture supernatant and cells were harvested at various time points. Cells and supernatants were frozen and thawed three times, followed by sonication in a cup horn sonicator. Cell lysates and supernatants were either mixed together or analyzed separately for virus titers using the virus plaque assay. VV-EGFP was used to monitor viral gene expression in MDMs, except cells were cultured for a short period (6 h) to allow EGFP expression only. At 6 h of culture, cells were fixed with 2% PFA, and EGFP-positive cells were quantitated using FACS. For VACV binding assays, primary MDMs were chilled to 4°C and incubated with vA5L-YFP at an MOI of 5 on ice for 30 min with gentle mixing (VACV binding condition). Cells were washed three times with ice-cold PBS and fixed with 2% PFA, and YFP-positive cells were quantitated using FACS.

Macrophage activation and RT-PCR transcriptional profiling. MDMs were activated using different cytokine combinations. First, isolated blood monocytes were cultured in complete RPMI 1640 supplemented with either 50 ng/ml of rhGM-CSF or 50 ng/ml of rhM-CSF. After 7 days of differentiation, GM-CSF-induced MDMs (M1) were stimulated with 10 ng/ml of LPS plus 50 ng/ml of rhIFN-γ. M-CSF-induced MDMs (M2) were activated with either 10 ng/ml of rhIL-4 (M2a), 10 ng/ml of LPS plus 10 ng/ml of rhIL-1β (M2b), or 10 ng/ml of rhIL-10 (M2c). Cells were cultured for 24 h. For inhibition of Jak2/Stat3 during M2c activation, 1 to 5 μM cucurbitacin I (JSI-124; Sigma-Aldrich, St. Louis, MO) was added along with rhIL-10. For reverse transcription-PCR (RT-PCR) analysis of activation-associated genes, cells were washed three times with PBS and subjected to RNA extraction using an RNeasy minikit (Qiagen, Hilden, Germany) according to the manufacturer's instructions. RNA was subjected to cDNA synthesis using the Superscript III first-strand synthesis kit (Life Technologies, Carlsbad, CA) according to the manufacturer's instructions. Real-time RT-PCR was performed using the RT^2 SYBR green/ROX FAST master mixes (Qiagen, Hilden, Germany) with primers against M1- or M2-specific genes, including the following: IL-6 forward, 5′-GAGGATACCATCCCAACAGACC-3′; IL-6 reverse, 5′-AAGTGCATCATCGTTGTTCATACA-3′; IL-10 forward, 5′-GCCTAACATGCTTCGAGA-3′; IL-10 reverse, 5′-TGATGTCTGGGTCTTGGTTC-3′; CD163 forward, 5′-CCAGTCCCAAACACTGTC-3′; CD163 reverse, 5′-TTCTGGAATGGTAGGCCTTG-3′; Arg1 forward, 5′-CAGAAGAATGGAAGAGTCAG-3′; Arg1 reverse, 5′-CAGATATGCAGGGAGTCACC-3′; β-actin forward, 5′-CTCGACACCAGGGCGTTAG-3; and β-actin reverse, 5′-CCACTCCATGCTCGATAGAT-3′ (Life Technologies, Carlsbad, CA). Expression data by the cycle threshold (C_T) value was compared to actin expression and analyzed using the $2^{-\Delta\Delta CT}$ method as previously described (31). For infection of activated cells, M1- or M2-polarized cells were infected with VACV WR at an MOI of 5 for 3 h. Cells were washed extensively with PBS and then cultured in medium containing activation cytokines.

CsCl density gradient ultracentrifugation for VACV separation. Virus-containing supernatant and cell pellet were harvested from 5 × 10^7 VACV-infected M2 macrophages. To separate and analyze mature versus enveloped virus particles, virus was purified from cell lysates via 24 to 40% sucrose gradients. Purified virus was added to CsCl gradients made with 2 ml of 1.30 g/ml overlaid with 3 ml of 1.25 g/ml, followed by 4 ml of 1.20 g/ml in a 12-ml tube, as previously described (32, 33), and spun in an Optima LE-80K ultracentrifuge with an SW-41 rotor (Beckman Coulter, Brea, CA) for 2 h at 120,000 × *g* (32,000 rpm) at 20°C. Fractions (0.5 ml of each) were harvested from the top of each gradient and subjected to virus collection by ultracentrifugation at 21,000 × *g* (15,000 rpm) for 30 min in a tabletop microcentrifuge. Virus pellets were resuspended in 100 μl of PBS and sonicated with a cup horn sonicator. The absorbance of each fraction was measured at 260 nm, and the number of virion particles was estimated using the following calculation: numbers of virus particles = $A_{260} \times (1.2 \times 10^{10})$.

Signaling pathway inhibition in human primary macrophages. M2-polarized MDMs were infected with VACV WR at an MOI of 5 for 3 h. Cells were washed three times with PBS and incubated in complete RPMI with 5 to 40 μM Akt inhibitor LY294002 or 1 to 100 μM Erk inhibitor PD98059. After incubation for 24 to 48 h, cells or supernatants were subjected to virus extraction to determine virus titers using the virus plaque assay. Cell lysates were also subjected to enzyme-linked immunosorbent assays (ELISAs) to determine the degree of signaling reduction by inhibitors using the Pathscan phospho-Akt1 and Pathscan phospho-p44 mitogen-activated protein kinase (MAPK) sandwich ELISA kits (Cell Signaling Technology, Danvers, MA) according to the manufacturer's instructions. With the same kits, Abs against Akt and Erk (Cell Signaling Technology) were used to detect levels of total Akt and Erk, respectively.

Confocal microscopy. MDMs were infected with vA5L-YFP VACV at an MOI of 5 and fixed at various intervals. To stain extracellular virions, cells were stained with rabbit polyclonal antiserum NR-565 against VACV WR A33 (NIH Biodefense and Emerging Infections Research Resources Repository, NIAID, NIH), followed by secondary Ab of goat anti-mouse IgG H+L conjugated to Alexa Fluor 546 (Life Technologies, Carlsbad, CA). In a separate condition, infected cells were fixed with 2% PFA, permeabilized with 0.1% saponin, and incubated with phalloidin conjugated with Alexa Fluor 546 (Life Technologies, Carlsbad, CA) for F-actin staining. Cells were then mounted onto glass slides using ProLong Gold antifade reagent (Life Technologies, Carlsbad, CA) containing 4′,6-diamidino-2-phenylindole (DAPI) dye for DNA staining. Slides were viewed using an Olympus FV1000-MPE confocal/multiphoton microscope fitted with a 60× water objective. Images were processed using ImageJ software (version 1.47; NIH, Bethesda, MD).

Statistical analysis. Data obtained from two groups were analyzed using the Student's *t* test, while data obtained from three groups or more were analyzed using Tukey's post hoc analysis of variance (ANOVA) test. Values of $P < 0.05$ were considered statistically significant.

RESULTS

VACV replicated in M1- and M2-polarized, but not human AB serum-derived, macrophages. It has been previously reported that VACV exhibits an abortive infection in primary human MDMs derived from peripheral blood monocytes by culturing them in medium containing 10% human AB serum (11). We infected human AB serum-derived MDMs with VACV WR at an MOI of 5 for 3 h to 48 h and found that VACV did not replicate, as virus plaque numbers did not increase (Fig. 1A), corroborating the previous report (11). Compared to MDM generated with human AB serum, it is known that supplementation of medium with GM-CSF or M-CSF was found to generate M1- or M2-polarized cells, respectively, and promote cell survival (34). After deriving

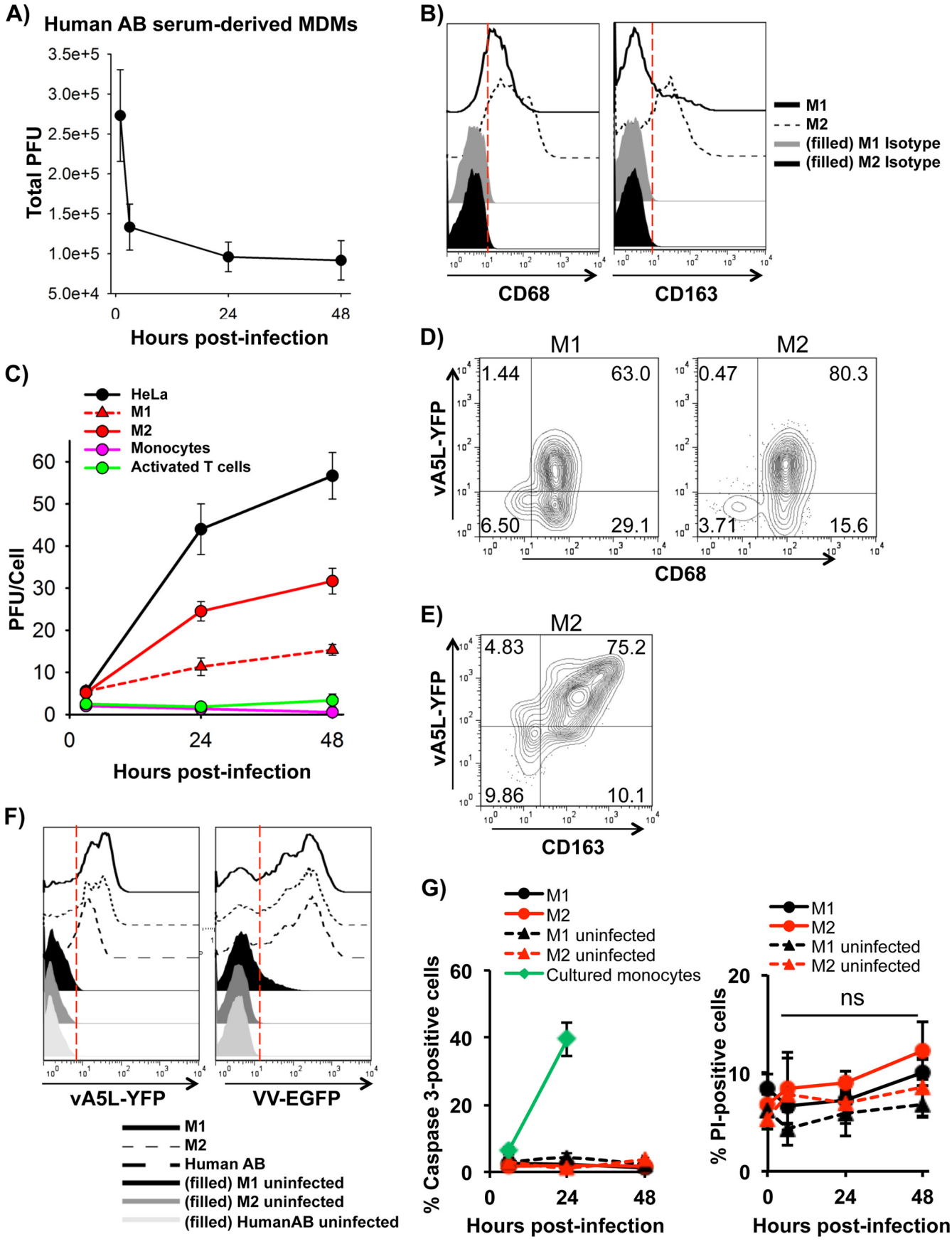
A)
Human AB serum-derived MDMs
Total PFU
3.5e+5
3.0e+5
2.5e+5
2.0e+5
1.5e+5
1.0e+5
5.0e+4
0
24
48
Hours post-infection
B)
M1
M2
(filled) M1 Isotype
(filled) M2 Isotype
CD68
CD163
C)
HeLa
M1
M2
Monocytes
Activated T cells
PFU/Cell
60
50
40
30
20
10
0
0
24
48
Hours post-infection
D)
M1
M2
vA5L-YFP
1.44
63.0
6.50
29.1
0.47
80.3
3.71
15.6
CD68
E)
M2
vA5L-YFP
4.83
75.2
9.86
10.1
CD163
F)
vA5L-YFP
VV-EGFP
M1
M2
Human AB
(filled) M1 uninfected
(filled) M2 uninfected
(filled) HumanAB uninfected
G)
M1
M2
M1 uninfected
M2 uninfected
Cultured monocytes
% Caspase 3-positive cells
60
40
20
0
0
24
48
Hours post-infection
M1
M2
M1 uninfected
M2 uninfected
ns
% PI-positive cells
20
10
0
0
24
48
Hours post-infection

MDMs with these cytokines, both M1- and M2-polarized MDMs expressed the low-density lipoprotein (LDL)-binding glycoprotein CD68, a common macrophage marker, while only M-CSF-polarized cells markedly expressed the scavenger receptor CD163, a surface marker for M2 MDMs (Fig. 1B). In contrast to MDMs derived from human AB serum, GM-CSF- and M-CSF-derived MDMs were permissive to VACV infection and replication (Fig. 1C). At an MOI of 5, GM-CSF-polarized cells produced 11.3 ± 2.1 virions per cell at 24 h and 15.3 ± 1.2 virions per cell at 48 h. M-CSF-polarized cells produced 24.5 ± 2.3 virions per cell at 24 h and 31.7 ± 3.1 virions per cell at 48 h. In comparison, HeLa cells, a human epithelial carcinoma cell line widely used for VACV infection and replication, produced 44.0 ± 6.0 virions per cell at 24 h and 56.7 ± 5.5 virions per cell at 48 h. Primary T cells activated with anti-CD3 and anti-CD28 Abs were also productive, as previously reported (35), but only produced 1.8 ± 0.8 virions per cell at 24 h and 3.3 ± 1.5 virions per cell at 48 h (Fig. 1C). Thus, VACV replicates in primary human M1 and M2 cells and relatively less efficiently in activated T cells, but it does not replicate in human AB serum-derived MDMs. After 24 h of infection with vA5L-YFP, expression of the late viral protein A5L was almost exclusively found on $CD68^+$ cells for both M1- and M2-polarized MDMs (Fig. 1D). Under the same conditions, CD163 surface expression was highly correlative to A5L expression in M2-polarized MDMs (Fig. 1E).

To understand whether the different degrees of VACV replication in the three types of MDMs (M1-, M2-, and human AB serum-derived MDMs) are directly related to efficacy of virus binding to and infection of these cell types, MDMs were incubated with vA5L-YFP under binding conditions (on ice for 30 min) or infected with VV-EGFP, a VACV WR strain containing an EGFP reporter gene regulated under a VACV early/late promoter, for a short period (<6 h; early infection). YFP-positive or EGFP-positive cells were quantitated by FACS. No significant differences in either virus binding or early infection were observed among these three MDM types (Fig. 1F), suggesting that VACV binding and early infection is comparable among human GM-CSF-, M-CSF-, and AB serum-derived cells. VACV infection was previously reported to induce apoptosis in murine macrophage cell line J774.G8 (36). To investigate the fates of VACV infection in primary human cells, apoptosis was monitored by intracellular staining of active caspase-3. No significant levels of caspase-3-positive MDMs were detected, and the levels did not increase within 2 days of VACV infection (Fig. 1G). This result was in contrast to those for uninfected primary human monocytes that underwent spontaneous apoptosis in *in vitro* culture (37) (Fig. 1G). Additionally, infected MDMs were stained with propidium iodide (PI) to detect necrotic cells, and no increase in PI-positive cells was observed (Fig. 1G). This result was concordant with observations that cell numbers were never significantly decreased throughout the 2-day infection and no nucleosomal units or apoptotic bodies were observed throughout extensive viewing by confocal microscopy (data not shown). It is notable that detection of surface phosphatidylserine with annexin V was not an appropriate assay for this experiment, as VACV was found to express phosphatidylserine on the virion surface (38, 39). We found that most cells were positive for annexin V staining after virus binding and throughout the infection (data not shown). Therefore, MDMs derived from human AB serum, GM-CSF, or M-CSF treatment have a similar degree of viral binding and early infection and do not undergo apoptosis within 2 days of infection.

Virus factories, actin tails, and branching structures formed in VACV-infected macrophages. Virus factories (also known as virosomes) and actin tails are well documented in VACV-infected cell lines and could not be detected in infected primary DCs, as these DCs are not permissive for VACV replication (17). To further investigate the cellular effects of VACV infection and replication in MDMs, we searched for the presence of these common structures associated with VACV-infected cell lines. At various stages of vA5L-YFP infection, monocytes or M2-polarized MDMs were visualized using confocal microscopy. In addition, F-actin was stained with phalloidin conjugated to the fluorophore Alexa Fluor 647 to observe actin dynamics throughout the infection. In agreement with the results obtained from the virus plaque assay, primary monocytes showed no visible increase in VACV particles after 24 h of infection (Fig. 2A). In contrast, VACV replication in MDMs was apparent, as numbers of cell-associated virions were increased (Fig. 2B). Characteristically, VACV infection in cell lines such as HeLa cells leads to the formation of perinuclear virus factories that coopt a section of the endoplasmic reticulum (ER) for VACV DNA replication and initial virus assembly (40). After 24 h of infection, perinuclear VACV factory structures with high levels of A5L expression were observed in M2-polarized MDMs (Fig. 2C) but not in monocytes (Fig. 2A). These perinuclear factory structures in M2 MDMs exhibited DAPI staining, indicating VACV DNA replication (Fig. 2C).

CEV virions in cell lines protrude from the cell surface via actin polymerization (41). This process requires certain host factors, such as Abl tyrosine kinases (42) and the products of VACV genes A36, A33, A34, and B5R (8). We found that VACV virions associated with actin tails in MDMs became visible by 3 h postinfection and persisted throughout the course of infection (Fig. 2D). Additionally, VACV virions were frequently observed to congregate inside projections linking neighboring cells together and in areas with lamellipodia-associated protrusions (Fig. 2B, white arrows, and E). Virus-induced branching between cells also occurred (Fig. 2B and F), which is reminiscent of the elongation and branching observed in infected cell lines, such as BS-C-1 (43). The VACV-associated lamellipodia and branching may represent a strategy for cell-to-cell transmission which can be visualized by live imaging assays. VACV-associated branching structures, actin tails, and virus factories were also observed in infected M1-polarized

FIG 1 VACV replicated in M1- and M2-polarized macrophages. MDMs derived from treatment of human AB serum (A), GM-CSF (C), or M-CSF (C) were infected with VACV WR at an MOI of 5, and virions were harvested from cell lysates at 3, 24, and 48 h of postinfection for the virus plaque assay. (B) MDMs were subjected to surface staining and FACS to measure human macrophage marker CD68 and M2-specific marker CD163. (D and E) M1- and M2-polarized MDMs infected withvA5L-YFP at an MOI of 5 for 24 h were stained for surface CD68 (D) or CD163 (E) and analyzed by FACS. (F) The degrees of VACV binding to and early infection of MDM subtypes were determined by FACS. MDM subtypes were incubated with vA5L-YFP at an MOI of 5 on ice for 30 min or with VV-EGFP at an MOI of 5 for 6 h and then subjected to FACS to determine the efficacy of VACV binding and early infection. (G) Apoptosis and necrosis of infected monocytes and MDMs were detected using intracellular caspase-3 staining and PI staining, respectively, at 6 h, 24 h, and 48 h postinfection. All data are representative of cells derived from five blood donors. ns, not significant.

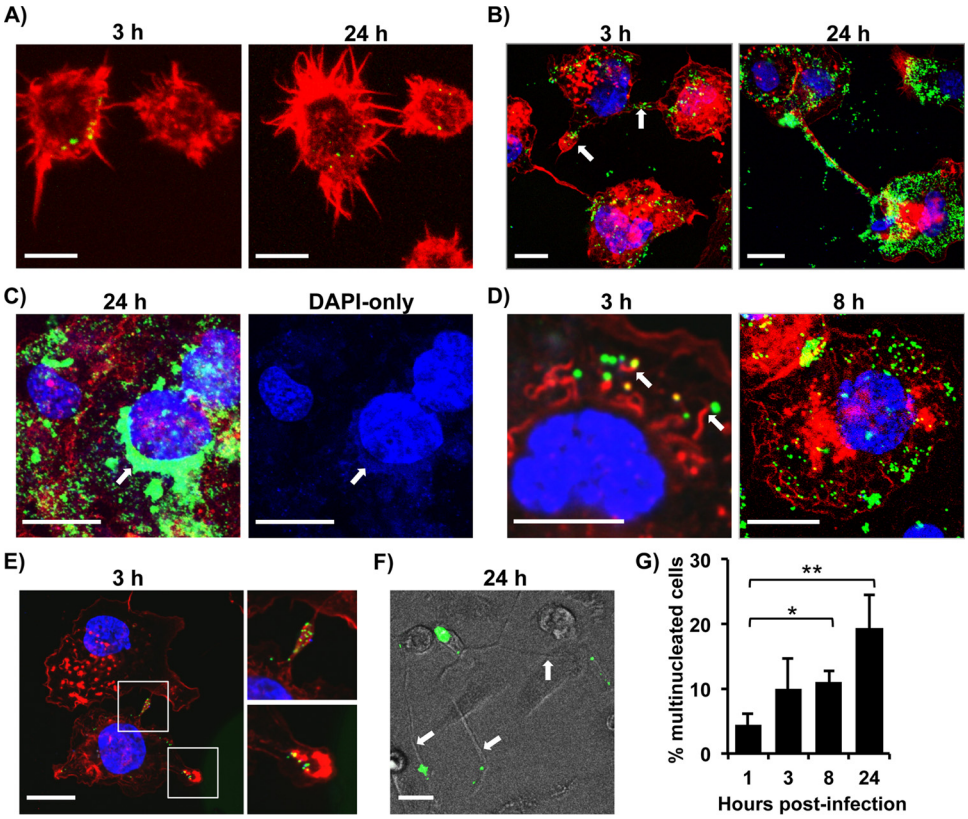

FIG 2 Virus factories, actin tails, and branching structures formed in VACV-infected macrophages. Primary monocytes (A) and M2-polarized MDMs (B to F) were infected with vA5L-YFP (green) at an MOI of 5 for various times as indicated and visualized along with F-actin staining with phalloidin (red) and DNA staining with DAPI (blue). Micrographs exhibited common structures found throughout infection, namely lamellipodia and branching (B, E, and F), virus factories (C), and actin tails (D). (F) Virus-associated branching structures were also viewed via transillumination. (G) Giant cell formation throughout VACV infection was observed, and multinucleated cells were counted at various time points. Scale bars represent 10 μM. All data are representative of cells derived from five blood donors. *, $P < 0.05$; **, $P < 0.01$.

MDMs (data not shown). The increasing presence of multinucleated cells was also evident over the course of infection. Macrophages typically fuse together to form multinucleated cells (giant cells), and this process is associated with granulomas and may occur in response to the presence of foreign bodies and certain pathogens. We found that 4.5% ± 1.6% ($n = 6$) of cells were multinucleated at the start of infection, which increased to 19.4% ± 5.0% ($n = 6$) after 24 h of infection (Fig. 2G). Together, our data indicate that VACV factory formation and VACV-associated actin tails occur in infected primary MDMs but not in primary monocytes. Additionally, VACV dissemination may occur through routes of cell-to-cell transmission via actin tails, lamellipodia, or branching structures.

MDMs mainly produced enveloped forms of VACV. When we used the virus plaque assay to measure VACV titers in culture supernatants and cell pellets from infected M1- and M2-polarized MDMs, we found that supernatants contained more infectious virions than did cell lysates (Fig. 3A), with 3-fold and 5-fold higher numbers of PFU than those in cell lysates of M1 and M2, respectively. Given that VACV infection for 2 days did not cause significant cell apoptosis and death to release IMV virions into the culture supernatants, our result suggests that most virions produced in MDMs are in the form of EEV. The cell-associated virions titrated by the virus plaque assay could either be IMV within the cell, CEV attached to the cell surface, EEV bound to the cell surface, or virus particles from the input of the primary infection. The proportion of intracellular versus extracellular cell-associated virus was determined by confocal microscopy using vA5L-YFP with Ab staining of surface VACV envelope protein A33. By this approach, intact virus particles inside or outside the cells can be visualized with vA5L-YFP, while cell surface-attached virions are seen by A33 staining of vA5L-YFP virions. For the first 3 h of infection, 5.7% ± 4.9% of cell-associated virions were CEV/EEV (Fig. 3B, yellow merged from A33 red stain and vA5L-YFP green stain, and C), which most likely were left over from the primary virus input. By 24 h of infection, the total number of virions greatly increased and the percentage of CEV/EEV rose to 28.9% ± 16.7% (Fig. 3B and C). By 48 h, the majority of cell-associated virions were CEV/EEV, at 68.6% ± 11.0% (Fig. 3B and C). These data suggest that, by 48 h of infection, the majority of cell-associated virions measured in Fig. 3A is in the CEV or reattached EEV form.

To analyze the proportion of enveloped versus mature VACV forms, virions were collected from cells and supernatants, purified, combined, and separated by a CsCl density gradient ultracentrifugation. The CsCl density gradient is able to separate enveloped virions (EV) (including EEV and CEV) that have a lower buoyant density corresponding to 1.23 to 1.24 g/ml CsCl in a continuous gradient from single-membrane IMV particles that have a higher buoyant density of 1.27 to 1.28 g/ml (44). For M2

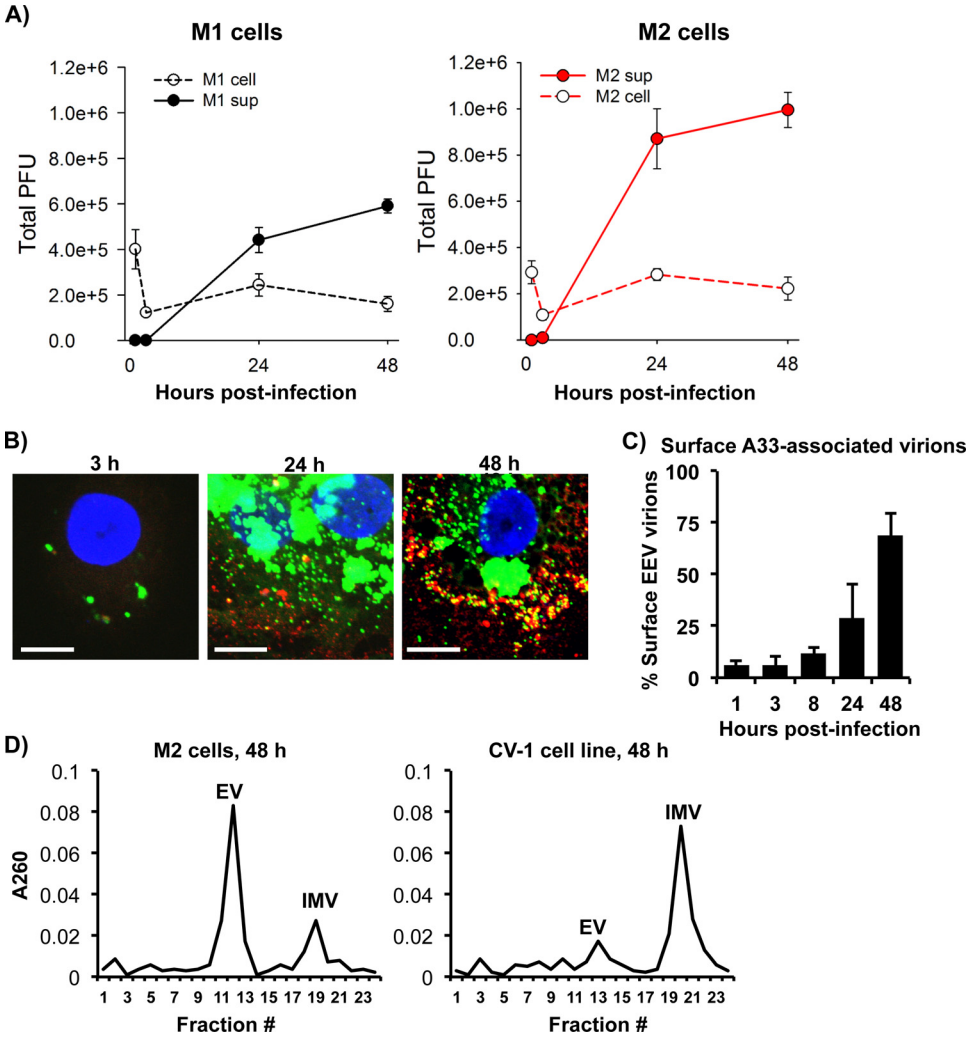

FIG 3 MDMs mainly produced enveloped forms of VACV. (A) M1- and M2-polarized MDMs were infected with VACV WR at an MOI of 5. Virions were extracted from either infected cells or culture supernatant (sup) at 3 h, 24 h, and 48 h postinfection and subjected to virus titration using the virus plaque assay. (B) M2-polarized cells were infected with vA5L-YFP (green) at an MOI of 5 for various times as indicated and then subjected to surface staining of VACV envelope protein A33 (red) with confocal microscopy analysis. Scale bars represent 10 μM. (C) The number of extracellular (vA5L-YFP plus A33 staining) and intracellular (vA5L-YFP only) cell-associated virions were counted at different time points as indicated. (D) Purified VACV particles from VACV WR-infected M2-polarized cells and CV-1 cells were extracted from cell lysates and supernatants and analyzed by separation on a CsCl density gradient. Fractions from the gradients were tested for absorbance at 260 to estimate the amount of virus particles corresponding to the buoyant densities of mature or enveloped forms of VACV. All data are representative of cells derived from five blood donors. EV, enveloped virus; IMV, intracellular mature virus.

cells, analysis of fractions from the gradient revealed that most virus particles were enriched in the fraction associated with EV buoyant density (Fig. 3D), with an estimated 3.8 times the number of VACV particles calculated in the IMV form. This is in contrast to VACV virions that are produced by the CV-1 cell line (Fig. 3D), with an estimated 4.1-fold higher number of IMV relative to fractions associated with EV. This result from infected CV-1 cells is typical of most cell lines infected with VACV WR. Overall, our results indicate that VACV produced in MDMs is mainly EEV released into the supernatant, and that by 48 h of infection most cell-associated VACV is CEV/EEV.

VACV-associated signaling pathways were required for virus replication in MDMs. VACV is dependent on Akt and Erk1/2 signaling pathways for entry and replication (45–48). Since we have discovered that M1 and M2 cells are permissive to VACV, we sought to analyze the dependence of these two pathways on VACV replication in MDMs independent of binding and entry. M2-polarized cells were infected with VACV at an MOI of 5 for 3 h and then treated with various concentrations of the Akt inhibitor LY294002 and the Erk1/2 inhibitor PD98059. LY294002 reduced the amount of pAkt and PD98059 reduced the amount of pErk1/2 in a dose-dependent manner (Fig. 4A). We found that both inhibitors reduced virus replication in a dose-dependent manner (Fig. 4B), suggesting that Akt and Erk pathways play a critical role in VACV replication in MDMs, which is in agreement with the results obtained from VACV infection in cell lines. Interestingly, the effects of both GM-CSF and M-CSF on MDM differentiation and maturation rely on activation of the Akt and Erk pathways.

Effects of macrophage activation on VACV replication. In general, classical (M1) activation of macrophages in response to

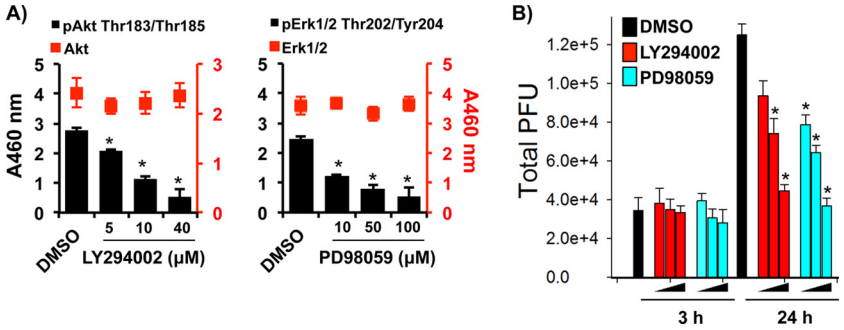

FIG 4 VACV-associated signaling pathways were required for VACV replication in MDMs. M2-polarized MDMs were infected with VACV WR at an MOI of 5 for 3 h. Cells were washed and treated with either 5 μM, 10 μM, or 40 μM LY294002 (Akt inhibitor) or 1 μM, 10 μM, or 100 μM PD98059 (Erk inhibitor). Cell lysates were collected at 3 h, 24 h, and 48 h postinfection. DMSO, dimethylsulfoxide. (A) Lysates were analyzed by a sandwich ELISA coated with anti-Akt or anti-Erk1/2 Abs and treated with secondary Abs against pAkt, pErk, or total target proteins. (B) Virions were extracted from cellular lysates at the time points indicated and titrated by the virus plaque assay. All data are representative of cells derived from five blood donors. *, $P < 0.05$.

IFN-γ and LPS stimulation exhibits an inflammatory phenotype. Alternative (M2) activation of macrophages can be induced via a variety of cytokines and reagents, including LPS, immune complexes, glucocorticoids, IL-1β, IL-10, transforming growth factor beta (TGF-β), and Th2 cytokines, such as IL-4 and IL-13. These cytokines and reagents can produce different cell types with unique functions. To further probe the unique macrophage-related pathways related to VACV infection in MDMs, M1 and M2 activations were induced to observe the effects on virus replication. Activation effects on infection may implicate specific macrophage-associated signaling pathways that are critical for VACV infection and may simulate the infection of these cells as they exist *in vivo*. M1-polarized cells activated by LPS and IFN-γ and M2-polarized cells activated by either IL-4 (M2a), LPS plus IL-1β (M2b), or IL-10 (M2c) for 2 days were analyzed with RT-PCR for common M1 and M2 activation markers. M1 activation exhibited higher levels of IL-6 mRNA associated with classical activation, while M2-activated cells had higher mRNA levels of arginase 1 (Arg-1), CD163, and IL-10 (Fig. 5A) associated with alternative activation. In addition, LPS-plus-IFN-γ-treated cells expressed higher levels of the M1 activation marker CD86 on the cell surface (Fig. 5B). M1- or M2-polarized cells were infected with VACV WR at an MOI of 5 for 3 h and then subjected to cell activation. Activation of M1-polarized cells with LPS plus IFN-γ had no effect on VACV replication, as VACV plaque numbers were not affected (Fig. 5C). Similarly, activation of M2-polarized cells by IL-4 had no effect on VACV replication, but treatment with LPS plus IL-1β or with IL-10 significantly reduced VACV productivity (Fig. 5C). At 48 h of infection, activation of M2b and M2c reduced VACV plaques from $1.22 \times 10^6 \pm 0.13 \times 10^6$ in M2-polarized cells to $0.55 \times 10^6 \pm 0.06 \times 10^6$ and $0.20 \times 10^6 \pm 0.05 \times 10^6$, respectively.

In T cells and macrophages, it has been shown that the downstream effects from IL-10 receptor activation largely act through the Jak/Stat pathway with Stat3 as a prominent transcription factor. We used cucurbitacin I, a specific inhibitor of Jak2/Stat3, to probe the effect of Stat3 activation on VACV replication. Compared to untreated M2 cells, M2c cells had significantly higher levels of pStat Y705 as determined by FACS, indicating IL-10 activates Stat3. Both M2-polarized and M2c cells treated with cucurbitacin I had reduced levels of activated Stat3 (Fig. 5D). When M2c cells were infected with VACV WR at an MOI of 5 for 3 h, followed by addition of cucurbitacin I, VACV production increased to the level of M2 cells without IL-10 stimulation (Fig. 5E). For example, infected M2 cells treated with IL-10 for 48 h produced $0.5 \times 10^6 \pm 0.2 \times 10^6$ PFU, while cells treated with IL-10 plus 5 μM cucurbitacin I produced $1.4 \times 10^6 \pm 0.1 \times 10^6$ PFU. Surprisingly, M2-polarized cells even without IL-10 treatment produced more VACV in response to the inhibitor treatment (Fig. 5E). After 48 h of incubation, untreated M2-polarized cells produced $1.3 \times 10^6 \pm 0.1 \times 10^6$ PFU, while cells treated with 5 μM cucurbitacin I produced $1.8 \times 10^6 \pm 0.1 \times 10^6$ total PFU. Overall, these data demonstrate that M1 or M2a activation has no effect on VACV replication, but M2b and M2c activation markedly reduces virus production. With M2c activation, a Jak2/Stat3 inhibitor rescued virus production to levels comparable to those of cells without IL-10 treatment.

DISCUSSION

The primary human cell types, including epithelial cells, keratinocytes, and fibroblasts in the airway, skin, and other tissues, have been considered the main workhorse for orthopoxvirus infection and replication. In one report, primary human dermal microvascular endothelial cells (HMVEC), fibroblasts, and keratinocytes were infected *in vitro* with VACV WR at an MOI of 10 for 60 h and produced 197.8, 129.1, and 21.8 PFU/cell, respectively (18). The result is comparable to our data where, after 48 h of infection, M1-polarized MDMs produced 15.3 ± 1.2 PFU/cell and M2-polarized cells produced 31.7 ± 3.1 PFU/cell when VACV was used at an MOI of 5 (Fig. 1C), suggesting that macrophages are a significant source of viral load *in vivo*. Previously, the only primary human leukocyte type known to be permissive to VACV was activated T cells (35). Among primary human leukocyte subtypes, VACV is able to bind to monocytes, activated T cells, B cells, and neutrophils (35, 49, 50), but it is able to express only viral genes in monocytes and activated T cells to a significant degree (49, 51, 52). Primary human monocytes and B cells have been shown to express little or no VACV late gene A56 (35), suggesting that these cell types are abortive. We have corroborated this result by showing no virus production in primary human monocytes using the virus plaque assay. In contrast to monocytes, MDMs derived from GM-CSF or M-CSF are permissive to VACV, but MDMs derived from human AB serum alone are abortive (Fig. 1A and C). In comparison to human AB serum alone, it is known that GM-CSF or M-CSF supplementation promotes survival of MDMs (34),

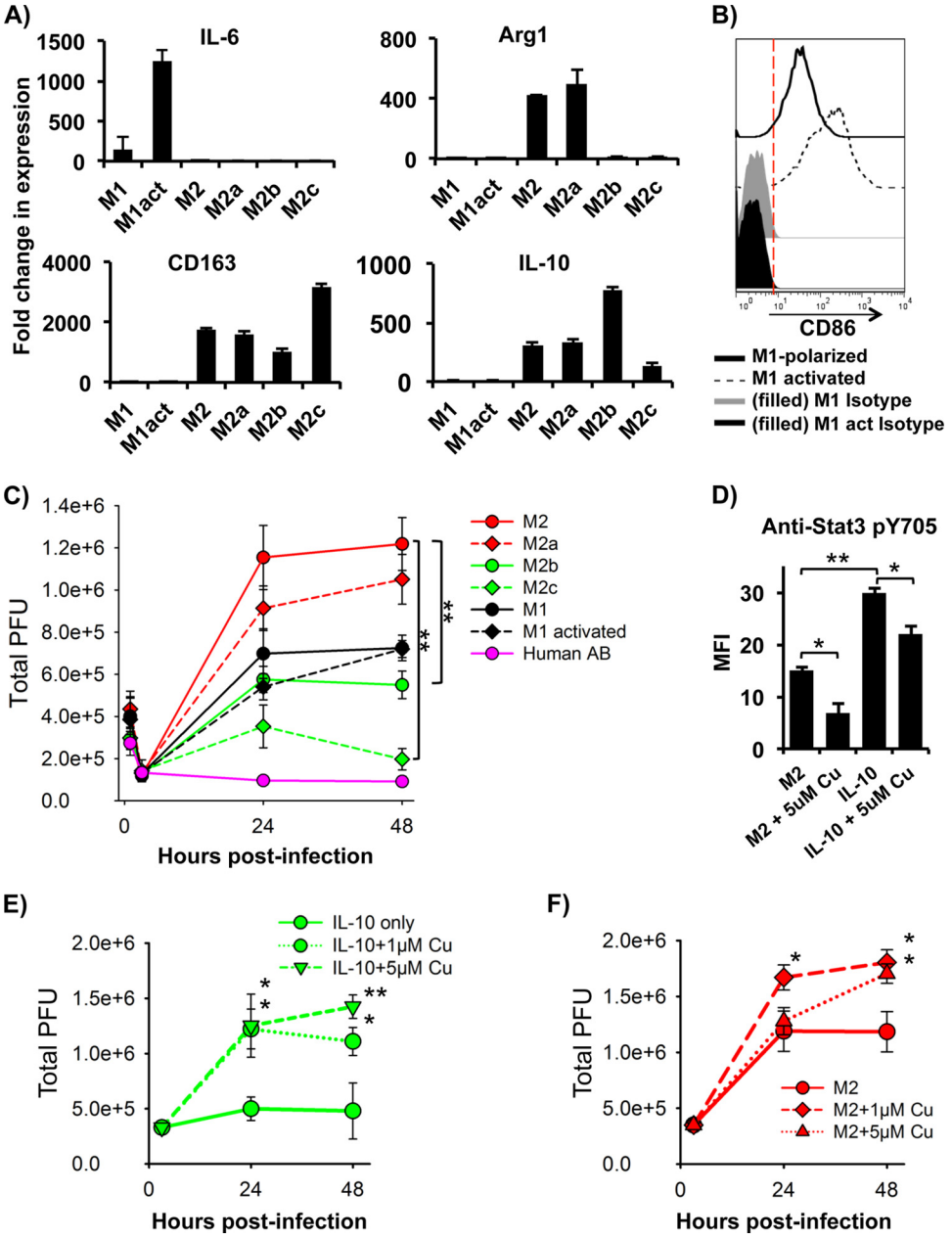

FIG 5 Effects of macrophage activation on VACV replication. M1-polarized cells were infected with VACV WR at an MOI of 5 for 3 h and then stimulated with LPS plus IFN-γ. M2-polarized cells were infected with VACV WR at an MOI of 5 for 3 h and then were stimulated with IL-4 (M2a), LPS plus IL-1β (M2b), or IL-10 (M2c). (A) After 24 h of stimulation, total RNA was extracted from cells and then subjected to cDNA synthesis and RT-PCR to detect expression of activation-associated genes of M1 (IL-6) and M2 (Arg-1, CD163, and IL-10). (B) M1 activation marker CD86 on the surface of activated M1 cells was analyzed using FACS. (C) The virus plaque assay was used to titrate infectious virus copies in the cellular lysates of M1- or M2-polarized cells in the different activation states. (D) M2-polarized cells were stimulated with IL-10 with or without cucurbitacin I and then subjected to analysis of Stat3 activation by intracellular staining with anti-pStat3 Y705 and FACS. (E) The virus plaque assay was used to titrate infectious virus copies in the cell lysates from IL-10 or IL-10-plus-cucurbitacin I-treated cells after 3 h, 24 h, and 48 h of infection. All data are representative of cells derived from five blood donors. M1act, activated M1 cells; Cu, cucurbitacin I. *, $P < 0.05$; **, $P < 0.01$.

increases cell proliferation (53), increases tumoricidal activity (21), and alters the expression of certain cell surface markers (53). VACV-infected GM-CSF-derived MDMs (M1) produce about half the amount of infectious virions produced by M-CSF-derived cells (M2) (Fig. 1C). The mechanisms underlying this difference are not clear, but they may be related to biological functions of M1 cells versus M2 cells. M1 cells are well-known proinflammatory macrophages, whereas M2 cells are anti-inflammatory macrophages. M1 cells express proinflammatory cytokines (54, 55) and are inducible to produce antiviral factors, including IFN regulatory factors 4 and 5 (IRF-4 and IRF-5) (56). These proinflammatory cytokines and antiviral factors may contribute to the reduced VACV production in infected M1 macrophages. In fact, IFN treatment can greatly diminish VACV titers *in vivo* (57), despite the

fact that poxviruses have evolved numerous strategies to counter host antiviral responses (58). Thus, the IFN-related pathways may also contribute to the reduced viral titer observed from M1 macrophages.

M-CSF binds to cell surface colony-stimulating factor 1 (c-Fms) to trigger dimerization and subsequent autophosphorylation of tyrosine residues, which serve as binding sites for SH2 domains of signaling molecules (59). Ultimately, this leads to the activation of Erk1/2, p38 MAPK, and Akt to promote monocyte survival and differentiation (60–65). GM-CSF receptor activation is followed by Jak2 phosphorylation of receptor tyrosines and eventual activation of Stat5 and the MAPK pathways via Grb2, Shc, and SHP2 (66). Similarly, VACV is reported to be dependent on MAPK signaling for replication (45, 46, 47). We observed significantly decreased viral production with treatment of Akt and Erk inhibitors (Fig. 4B), although the off-target effects of each inhibitor cannot be excluded. Even though the degree of this loss of virus production may not significant enough to be clinically relevant, this result demonstrates a similar sensitivity of VACV to signal transduction pathways previously shown in cell lines. VACV infection itself induces the activation of the Akt and Erk1/2 pathways in primary human monocytes (67), and viral protein production is dependent on activation of these pathways (67). Since monocytes are abortive to VACV infection, it is likely that the stimulation of these two pathways alone is not sufficient to induce permissiveness in monocytic cells. In primary T cells and T cell lines, tyrosine phosphorylation of CCR5 alone allows cells to become permissive to VACV replication (68, 69), and such a pathway may be significant for the induction of permissiveness in monocytic cells.

In vitro activation of MDMs in some ways reflects macrophage activation states *in vivo* in certain diseases (25, 27). The different macrophage activation states may alter susceptibility of these cells to virus infection and replication. For example, M1 and M2a activation inhibits HIV-1 replication through different mechanisms, and once activation is resolved, HIV-1 replication increases (70). We found that M1 activation resulted in no change to VACV production (Fig. 5C). This is counterintuitive because of the many antiviral factors induced with LPS and IFN-γ stimulation (71), although VACV has evolved dozens of strategies to evade such antiviral responses (72). This result may reflect how M1-polarized cells induced by VACV focus inflammation react to VACV infection *in vivo*. M2-polarized M-CSF-derived MDMs are considered a model for normal tissue macrophages (73, 74), as M-CSF is ubiquitously expressed in the blood and many tissues (75, 76). Alternative activation with IL-4 treatment had no detectable effect on VACV replication (Fig. 5C), which is consistent with similar transcriptional profiles of M-CSF-treated versus IL-4-treated MDMs (73). Thus, this result may model how M2-polarized or M2a tissue macrophages react to primary VACV infection *in vivo*. However, alternative activation with IL-10 or with LPS plus IL-1β significantly reduced virus production (Fig. 5C). M2b activation in macrophages is unique among the routes of alternative activation, because it induces IL-10 and low levels of IL-12, as well as high levels of inflammatory cytokines (77). This inflammatory response may induce expression of antiviral factors (such as type I IFNs) that contribute to the diminished levels of VACV production. In different cell types, many of the IL-10 effects are mediated via the activation of the Jak2/Stat3 pathway, with Stat3 being a crucial factor for alternative activation in macrophages and immune homeostasis. VACV infection does not block Stat3 activity but does dephosphorylate Stat1 to reduce the effect of IFN stimulation (78). In general, M1 activation involves Stat1 activation, while much of the effect of M2 activation centers on Stat6 (27). We found that the Jak2/Stat3 inhibitor cucurbitacin I increased VACV production in both M2-polarized and M2c-activated cells in a manner correlative to Stat3 activation (Fig. 5D to F).

M1 macrophages are critical components of the antitumor immune response. However, tumors and the environmental cues can polarize M1 toward the M2 phenotype that assists tumor growth (79). If macrophages are a significant source of viral titer *in vivo*, we believe the IL-10/Stat3-mediated reduction of VACV production is relevant to potential oncolytic VACV therapies. The efficacy of an oncolytic virus is determined not only by its ability to specifically target and kill tumor cells but also by its ability to propagate and spread efficiently among cells within a tumor. IL-10 produced by T regulatory cells in many types of cancer has been associated with a reduction of Th1 responses that regulate IFN-γ and $CD8^+$ cell antitumor immunity (80–82). This role of IL-10 as an anti-inflammatory agent in tumors is significant for the use of VACV as an oncolytic agent, as we have found that VACV replication in MDMs is sensitive to IL-10 stimulation. Our results suggest that cancer therapies diminishing the effects of IL-10 are complementary to oncolytic VACV therapy by boosting the viral titer and dissemination within a tumor. Our finding that MDMs produced an unusually large amount of EEV is also uniquely relevant for oncolytic VACV therapy, because the level of EEV in a tumor was found to be positively correlated with the effectiveness of treatment (83).

Our study also provides several lines of evidence that primary macrophages promote VACV dissemination: (i) high EEV production, (ii) actin tail-associated CEV, and (iii) VACV-associated cell branching and linkages. IMV is often considered the most abundant infectious form of VACV produced in most cell types. The CEV form of VACV mediates cell-to-cell spreading, and detachment of CEV to become EEV mediates longer-range dissemination (8, 84). We observed that by 48 h of infection with VACV WR, EEVs were the dominant virus form produced in MDMs (Fig. 3A and D). This principle is comparable to that for the rabbit kidney cell line RK-13, which produces significantly more EEV than other cell lines (85). Additionally, the VACV strain IHD-J produces high EEV titers in cell lines, especially in RK-13 (85). Compared to the VACV WR strain, IHD-J produces more EEV particles because it releases more CEV into the supernatant, while strains like VACV WR retain CEV on the cell surface (84). Thus, considering the paradigm in EEV production that exists between WR and IHD-J cell lines, this anomaly in MDMs will likely be explained by a host cell-related mechanism like that of RK-13 rather than a characteristic of the virus strain. In cell lines, different factors have been associated with EEV production, including the Abl tyrosine kinases (42, 86) and SH2 domain-containing phosphoinositide 5-phosphatase 2 (SHIP2) (87), which may be involved with the high EEV production seen in MDMs.

In conclusion, human primary macrophages are an additional leukocyte type that is permissive to VACV. After infection, these cells produce EEV for long-range dissemination and also form actin tails, cell linkages, lamellipodia, and branching structures associated with virions, which may contribute to cell-to-cell spread. Different macrophage subtypes and activation states affect VACV infection and replication. Therefore, macrophages may be

a significant source of viral load *in vivo* and promote long-range dissemination.

ACKNOWLEDGMENTS

We thank J. W. Yewdell and B. Moss at the NIH (Bethesda, MD) for VV-EGFP and vA5L-YFP.

This work was supported in part by a Grand Challenges Explorations (GCE) Phase II grant through the Bill & Melinda Gates Foundation (OPP1035237 to Q.Y.), NIH 1R21AI104268 (Q.Y.), the Showalter Research Trust Fund (Q.Y.), NIH T32 AI060519 (D.B.), the National Natural Science Foundation of Zhejiang Province (Y2110608 to N.H.), and the Research Facilities Improvement Program, grant number C06 RR015481-01, from the National Center for Research Resources, NIH, to Indiana University School of Medicine.

D.B. and Q.Y. designed and performed research, analyzed data, and wrote the paper. N.S., J.L., N.H., K.Y., and M.D. contributed vital new reagents and assisted with virus preparation.

We declare that we have no conflicts of interest.

REFERENCES

1. **Jahrling PB, Hensley LE, Martinez MJ, Leduc JW, Rubins KH, Relman DA, Huggins JW.** 2004. Exploring the potential of variola virus infection of cynomolgus macaques as a model for human smallpox. Proc. Natl. Acad. Sci. U. S. A. **101:**15196–15200. http://dx.doi.org/10.1073/pnas.0405954101.
2. **Wahl-Jensen V, Cann JA, Rubins KH, Huggins JW, Fisher RW, Johnson AJ, de Kok-Mercado F, Larsen T, Raymond JL, Hensley LE, Jahrling PB.** 2011. Progression of pathogenic events in cynomolgus macaques infected with variola virus. PLoS One **6:**e24832. http://dx.doi.org/10.1371/journal.pone.0024832.
3. **Tsuru S, Kitani H, Seno M, Abe M, Zinnaka Y, Nomoto K.** 1983. Mechanism of protection during the early phase of a generalized viral infection. I. Contribution of phagocytes to protection against ectromelia virus. J. Gen. Virol. **64**(Part 9)**:**2021–2026.
4. **Karupiah G, Buller RM, Van Rooijen N, Duarte CJ, Chen J.** 1996. Different roles for CD4+ and CD8+ T lymphocytes and macrophage subsets in the control of a generalized virus infection. J. Virol. **70:**8301–8309.
5. **Roberts JA.** 1964. Growth of virulent and attenuated ectromelia virus in cultured macrophages from normal and ectromeliaimmune mice. J. Immunol. **92:**837–842.
6. **Kochneva GV, Urmanov IH, Ryabchikova EI, Streltsov VV, Serpinsky OI.** 1994. Fine mechanisms of ectromelia virus thymidine kinase-negative mutants avirulence. Virus Res. **34:**49–61. http://dx.doi.org/10.1016/0168-1702(94)90118-X.
7. **Damon IK.** 2007. Poxviruses, p 2947–2976. *In* Knipe DM, Howley PM, Griffin DE, Lamb RA, Martin MA, Roizman B, Straus SE (ed), Fields virology, 5th ed. Lippincott Williams & Wilkins, Philadelphia, PA.
8. **Smith GL, Vanderplasschen A, Law M.** 2002. The formation and function of extracellular enveloped vaccinia virus. J. Gen. Virol. **83:**2915–2931. http://vir.sgmjournals.org/content/83/12/2915.
9. **Doceul V, Hollinshead M, van der Linden L, Smith GL.** 2010. Repulsion of superinfecting virions: a mechanism for rapid virus spread. Science **327:**873–876. http://dx.doi.org/10.1126/science.1183173.
10. **Hickman HD, Reynoso GV, Ngudiankama BF, Rubin EJ, Magadan JG, Cush SS, Gibbs J, Molon B, Bronte V, Bennink JR, Yewdell JW.** 2013. Anatomically restricted synergistic antiviral activities of innate and adaptive immune cells in the skin. Cell Host Microbe **13:**155–168. http://dx.doi.org/10.1016/j.chom.2013.01.004.
11. **Broder CC, Kennedy PE, Michaels F, Berger EA.** 1994. Expression of foreign genes in cultured human primary macrophages using recombinant vaccinia virus vectors. Gene **142:**167–174. http://dx.doi.org/10.1016/0378-1119(94)90257-7.
12. **Drillien R, Spehner D, Bohbot A, Hanau D.** 2000. Vaccinia virus-related events and phenotypic changes after infection of dendritic cells derived from human monocytes. Virology **268:**471–481. http://dx.doi.org/10.1006/viro.2000.0203.
13. **Engelmayer J, Larsson M, Subklewe M, Chahroudi A, Cox WI, Steinman RM, Bhardwaj N.** 1999. Vaccinia virus inhibits the maturation of human dendritic cells: a novel mechanism of immune evasion. J. Immunol. **163:**6762–6768.
14. **Jenne L, Hauser C, Arrighi JF, Saurat JH, Hugin AW.** 2000. Poxvirus as a vector to transduce human dendritic cells for immunotherapy: abortive infection but reduced APC function. Gene Ther. **7:**1575–1583. http://dx.doi.org/10.1038/sj.gt.3301287.
15. **Subklewe M, Chahroudi A, Schmaljohn A, Kurilla MG, Bhardwaj N, Steinman RM.** 1999. Induction of Epstein-Barr virus-specific cytotoxic T-lymphocyte responses using dendritic cells pulsed with EBNA-3A peptides or UV-inactivated, recombinant EBNA-3A vaccinia virus. Blood **94:**1372–1381.
16. **Bronte V, Carroll MW, Goletz TJ, Wang M, Overwijk WW, Marincola F, Rosenberg SA, Moss B, Restifo NP.** 1997. Antigen expression by dendritic cells correlates with the therapeutic effectiveness of a model recombinant poxvirus tumor vaccine. Proc. Natl. Acad. Sci. U. S. A. **94:**3183–3188. http://dx.doi.org/10.1073/pnas.94.7.3183.
17. **Chahroudi A, Garber DA, Reeves P, Liu L, Kalman D, Feinberg MB.** 2006. Differences and similarities in viral life cycle progression and host cell physiology after infection of human dendritic cells with modified vaccinia virus Ankara and vaccinia virus. J. Virol. **80:**8469–8481. http://dx.doi.org/10.1128/JVI.02749-05.
18. **Liu L, Xu Z, Fuhlbrigge RC, Pena-Cruz V, Lieberman J, Kupper TS.** 2005. Vaccinia virus induces strong immunoregulatory cytokine production in healthy human epidermal keratinocytes: a novel strategy for immune evasion. J. Virol. **79:**7363–7370. http://dx.doi.org/10.1128/JVI.79.12.7363-7370.2005.
19. **Musson RA.** 1983. Human serum induces maturation of human monocytes in vitro. Changes in cytolytic activity, intracellular lysosomal enzymes, and nonspecific esterase activity. Am. J. Pathol. **111:**331–340.
20. **Eischen A, Vincent F, Bergerat JP, Louis B, Faradji A, Bohbot A, Oberling F.** 1991. Long term cultures of human monocytes in vitro. Impact of GM-CSF on survival and differentiation. J. Immunol. Methods **143:**209–221.
21. **Suzu S, Yokota H, Yamada M, Yanai N, Saito M, Kawashima T, Saito M, Takaku F, Motoyoshi K.** 1989. Enhancing effect of human monocytic colony-stimulating factor on monocyte tumoricidal activity. Cancer Res. **49:**5913–5917.
22. **Helinski EH, Bielat KL, Ovak GM, Pauly JL.** 1988. Long-term cultivation of functional human macrophages in Teflon dishes with serum-free media. J. Leukoc. Biol. **44:**111–121.
23. **Vogel SN, Perera PY, Hogan MM, Majde JA.** 1988. Use of serum-free, compositionally defined medium for analysis of macrophage differentiation in vitro. J. Leukoc. Biol. **44:**136–142.
24. **Jaguin M, Houlbert N, Fardel O, Lecureur V.** 2013. Polarization profiles of human M-CSF-generated macrophages and comparison of M1-markers in classically activated macrophages from GM-CSF and M-CSF origin. Cell. Immunol. **281:**51–61. http://dx.doi.org/10.1016/j.cellimm.2013.01.010.
25. **Loke P, Nair MG, Parkinson J, Guiliano D, Blaxter M, Allen JE.** 2002. IL-4 dependent alternatively-activated macrophages have a distinctive in vivo gene expression phenotype. BMC Immunol. **3:**7. http://dx.doi.org/10.1186/1471-2172-3-7.
26. **Ghassabeh GH, De Baetselier P, Brys L, Noel W, Van Ginderachter JA, Meerschaut S, Beschin A, Brombacher F, Raes G.** 2006. Identification of a common gene signature for type II cytokine-associated myeloid cells elicited in vivo in different pathologic conditions. Blood **108:**575–583. http://dx.doi.org/10.1182/blood-2005-04-1485.
27. **Sica A, Mantovani A.** 2012. Macrophage plasticity and polarization: in vivo veritas. J. Clin. Investig. **122:**787–795. http://dx.doi.org/10.1172/JCI59643.
28. **Norbury CC, Malide D, Gibbs JS, Bennink JR, Yewdell JW.** 2002. Visualizing priming of virus-specific CD8+ T cells by infected dendritic cells in vivo. Nat. Immunol. **3:**265–271. http://dx.doi.org/10.1038/ni762.
29. **Katsafanas GC, Moss B.** 2007. Colocalization of transcription and translation within cytoplasmic poxvirus factories coordinates viral expression and subjugates host functions. Cell Host Microbe **2:**221–228. http://dx.doi.org/10.1016/j.chom.2007.08.005.
30. **Law M, Smith GL.** 2004. Studying the binding and entry of the intracellular and extracellular enveloped forms of vaccinia virus. Methods Mol. Biol. **269:**187–204. http://dx.doi.org/10.1385/1-59259-789-0:187.
31. **Livak KJ, Schmittgen TD.** 2001. Analysis of relative gene expression data using real-time quantitative PCR and the $2(-\Delta\Delta C_T)$ method. Methods **25:**402–408. http://dx.doi.org/10.1006/meth.2001.1262.
32. **Herrera E, Lorenzo MM, Blasco R, Isaacs SN.** 1998. Functional analysis of vaccinia virus B5R protein: essential role in virus envelopment is inde-

pendent of a large portion of the extracellular domain. J. Virol. **72:**294–302.
33. **Payne LG, Norrby E.** 1976. Presence of haemagglutinin in the envelope of extracellular vaccinia virus particles. J. Gen. Virol. **32:**63–72. http://dx.doi.org/10.1099/0022-1317-32-1-63.
34. **Young DA, Lowe LD, Clark SC.** 1990. Comparison of the effects of IL-3, granulocyte-macrophage colony-stimulating factor, and macrophage colony-stimulating factor in supporting monocyte differentiation in culture. Analysis of macrophage antibody-dependent cellular cytotoxicity. J. Immunol. **145:**607–615.
35. **Chahroudi A, Chavan R, Kozyr N, Waller EK, Silvestri G, Feinberg MB.** 2005. Vaccinia virus tropism for primary hematolymphoid cells is determined by restricted expression of a unique virus receptor. J. Virol. **79:**10397–10407. http://dx.doi.org/10.1128/JVI.79.16.10397-10407.2005.
36. **Humlova Z, Vokurka M, Esteban M, Melkova Z.** 2002. Vaccinia virus induces apoptosis of infected macrophages. J. Gen. Virol. **83:**2821–2832. http://vir.sgmjournals.org/content/83/11/2821.
37. **Fahy RJ, Doseff AI, Wewers MD.** 1999. Spontaneous human monocyte apoptosis utilizes a caspase-3-dependent pathway that is blocked by endotoxin and is independent of caspase-1. J. Immunol. **163:**1755–1762.
38. **Mercer J, Helenius A.** 2008. Vaccinia virus uses macropinocytosis and apoptotic mimicry to enter host cells. Science **320:**531–535. http://dx.doi.org/10.1126/science.1155164.
39. **Jemielity S, Wang JJ, Chan YK, Ahmed AA, Li W, Monahan S, Bu X, Farzan M, Freeman GJ, Umetsu DT, Dekruyff RH, Choe H.** 2013. TIM-family proteins promote infection of multiple enveloped viruses through virion-associated phosphatidylserine. PLoS Pathog. **9:**e1003232. http://dx.doi.org/10.1371/journal.ppat.1003232.
40. **Tolonen N, Doglio L, Schleich S, Krijnse Locker J.** 2001. Vaccinia virus DNA replication occurs in endoplasmic reticulum-enclosed cytoplasmic mini-nuclei. Mol. Biol. Cell **12:**2031–2046. http://dx.doi.org/10.1091/mbc.12.7.2031.
41. **Frischknecht F, Moreau V, Rottger S, Gonfloni S, Reckmann I, Superti-Furga G, Way M.** 1999. Actin-based motility of vaccinia virus mimics receptor tyrosine kinase signalling. Nature **401:**926–929. http://dx.doi.org/10.1038/44860.
42. **Reeves PM, Bommarius B, Lebeis S, McNulty S, Christensen J, Swimm A, Chahroudi A, Chavan R, Feinberg MB, Veach D, Bornmann W, Sherman M, Kalman D.** 2005. Disabling poxvirus pathogenesis by inhibition of Abl-family tyrosine kinases. Nat. Med. **11:**731–739. http://dx.doi.org/10.1038/nm1265.
43. **Sanderson CM, Way M, Smith GL.** 1998. Virus-induced cell motility. J. Virol. **72:**1235–1243.
44. **Boulter EA, Appleyard G.** 1973. Differences between extracellular and intracellular forms of poxvirus and their implications. Prog. Med. Virol. **16:**86–108.
45. **de Magalhaes JC, Andrade AA, Silva PN, Sousa LP, Ropert C, Ferreira PC, Kroon EG, Gazzinelli RT, Bonjardim CA.** 2001. A mitogenic signal triggered at an early stage of vaccinia virus infection: implication of MEK/ERK and protein kinase A in virus multiplication. J. Biol. Chem. **276:**38353–38360. http://dx.doi.org/10.1074/jbc.M100183200.
46. **Andrade AA, Silva PN, Pereira AC, De Sousa LP, Ferreira PC, Gazzinelli RT, Kroon EG, Ropert C, Bonjardim CA.** 2004. The vaccinia virus-stimulated mitogen-activated protein kinase (MAPK) pathway is required for virus multiplication. Biochem. J. **381:**437–446. http://dx.doi.org/10.1042/BJ20031375.
47. **Soares JA, Leite FG, Andrade LG, Torres AA, De Sousa LP, Barcelos LS, Teixeira MM, Ferreira PC, Kroon EG, Souto-Padron T, Bonjardim CA.** 2009. Activation of the PI3K/Akt pathway early during vaccinia and cowpox virus infections is required for both host survival and viral replication. J. Virol. **83:**6883–6899. http://dx.doi.org/10.1128/JVI.00245-09.
48. **Izmailyan R, Hsao JC, Chung CS, Chen CH, Hsu PW, Liao CL, Chang W.** 2012. Integrin beta1 mediates vaccinia virus entry through activation of PI3K/Akt signaling. J. Virol. **86:**6677–6687. http://dx.doi.org/10.1128/JVI.06860-11.
49. **Byrd D, Amet T, Hu N, Lan J, Hu S, Yu Q.** 2013. Primary human leukocyte subsets differentially express vaccinia virus receptors enriched in lipid rafts. J. Virol. **87:**9301–9312. http://dx.doi.org/10.1128/JVI.01545-13.
50. **Chan WM, Bartee EC, Moreb JS, Dower K, Connor JH, McFadden G.** 2013. Myxoma and vaccinia viruses bind differentially to human leukocytes. J. Virol. **87:**4445–4460. http://dx.doi.org/10.1128/JVI.03488-12.
51. **Yu Q, Hu N, Ostrowski M.** 2009. Poxvirus tropism for primary human leukocytes and hematopoietic cells. Methods Mol. Biol. **515:**309–328. http://dx.doi.org/10.1007/978-1-59745-559-6_22.
52. **Sanchez-Puig JM, Sanchez L, Roy G, Blasco R.** 2004. Susceptibility of different leukocyte cell types to vaccinia virus infection. Virol. J. **1:**10. http://dx.doi.org/10.1186/1743-422X-1-10.
53. **Finnin M, Hamilton JA, Moss ST.** 1999. Characterization of a CSF-induced proliferating subpopulation of human peripheral blood monocytes by surface marker expression and cytokine production. J. Leukoc. Biol. **66:**953–960.
54. **Fleetwood AJ, Lawrence T, Hamilton JA, Cook AD.** 2007. Granulocyte-macrophage colony-stimulating factor (CSF) and macrophage CSF-dependent macrophage phenotypes display differences in cytokine profiles and transcription factor activities: implications for CSF blockade in inflammation. J. Immunol. **178:**5245–5252. http://www.jimmunol.org/content/178/8/5245.
55. **Fleetwood AJ, Dinh H, Cook AD, Hertzog PJ, Hamilton JA.** 2009. GM-CSF- and M-CSF-dependent macrophage phenotypes display differential dependence on type I interferon signaling. J. Leukoc. Biol. **86:**411–421. http://dx.doi.org/10.1189/jlb.1108702.
56. **Lacey DC, Achuthan A, Fleetwood AJ, Dinh H, Roiniotis J, Scholz GM, Chang MW, Beckman SK, Cook AD, Hamilton JA.** 2012. Defining GM-CSF- and macrophage-CSF-dependent macrophage responses by in vitro models. J. Immunol. **188:**5752–5765. http://dx.doi.org/10.4049/jimmunol.1103426.
57. **Liu G, Zhai Q, Schaffner DJ, Wu A, Yohannes A, Robinson TM, Maland M, Wells J, Voss TG, Bailey C, Alibek K.** 2004. Prevention of lethal respiratory vaccinia infections in mice with interferon-alpha and interferon-gamma. FEMS Immunol. Med. Microbiol. **40:**201–206. http://dx.doi.org/10.1016/S0928-8244(03)00358-4.
58. **Smith GL, Benfield CT, Maluquer de Motes C, Mazzon M, Ember SW, Ferguson BJ, Sumner RP.** 2013. Vaccinia virus immune evasion: mechanisms, virulence and immunogenicity. J. Gen. Virol. **94:**2367–2392. http://dx.doi.org/10.1099/vir.0.055921-0.
59. **Downing JR, Rettenmier CW, Sherr CJ.** 1988. Ligand-induced tyrosine kinase activity of the colony-stimulating factor 1 receptor in a murine macrophage cell line. Mol. Cell. Biol. **8:**1795–1799.
60. **Hamilton JA.** 1997. CSF-1 signal transduction. J. Leukoc. Biol. **62:**145–155.
61. **Wang Y, Zeigler MM, Lam GK, Hunter MG, Eubank TD, Khramtsov VV, Tridandapani S, Sen CK, Marsh CB.** 2007. The role of the NADPH oxidase complex, p38 MAPK, and Akt in regulating human monocyte/macrophage survival. Am. J. Respir. Cell Mol. Biol. **36:**68–77. http://dx.doi.org/10.1165/rcmb.2006-0165OC.
62. **Bhatt NY, Kelley TW, Khramtsov VV, Wang Y, Lam GK, Clanton TL, Marsh CB.** 2002. Macrophage-colony-stimulating factor-induced activation of extracellular-regulated kinase involves phosphatidylinositol 3-kinase and reactive oxygen species in human monocytes. J. Immunol. **169:**6427–6434. http://www.jimmunol.org/content/169/11/6427.
63. **Sengupta A, Liu WK, Yeung YG, Yeung DC, Frackelton AR, Jr, Stanley ER.** 1988. Identification and subcellular localization of proteins that are rapidly phosphorylated in tyrosine in response to colony-stimulating factor 1. Proc. Natl. Acad. Sci. U. S. A. **85:**8062–8066. http://dx.doi.org/10.1073/pnas.85.21.8062.
64. **Platanias LC.** 2003. Map kinase signaling pathways and hematologic malignancies. Blood **101:**4667–4679. http://dx.doi.org/10.1182/blood-2002-12-3647.
65. **Cross M, Nguyen T, Bogdanoska V, Reynolds E, Hamilton JA.** 2005. A proteomics strategy for the enrichment of receptor-associated complexes. Proteomics **5:**4754–4763. http://dx.doi.org/10.1002/pmic.200500058.
66. **Guthridge MA, Stomski FC, Thomas D, Woodcock JM, Bagley CJ, Berndt MC, Lopez AF.** 1998. Mechanism of activation of the GM-CSF, IL-3, and IL-5 family of receptors. Stem Cells **16:**301–313. http://dx.doi.org/10.1002/stem.160301.
67. **Hu N, Yu R, Shikuma C, Shiramizu B, Ostrwoski MA, Yu Q.** 2009. Role of cell signaling in poxvirus-mediated foreign gene expression in mammalian cells. Vaccine **27:**2994–3006. http://dx.doi.org/10.1016/j.vaccine.2009.02.103.
68. **Rahbar R, Murooka TT, Fish EN.** 2009. Role for CCR5 in dissemination of vaccinia virus in vivo. J. Virol. **83:**2226–2236. http://dx.doi.org/10.1128/JVI.01655-08.
69. **Rahbar R, Murooka TT, Hinek AA, Galligan CL, Sassano A, Yu C, Srivastava K, Platanias LC, Fish EN.** 2006. Vaccinia virus activation of CCR5 invokes tyrosine phosphorylation signaling events that support vi-

rus replication. J. Virol. **80:**7245–7259. http://dx.doi.org/10.1128/JVI.00463-06.

70. **Cassol E, Cassetta L, Rizzi C, Alfano M, Poli G.** 2009. M1 and M2a polarization of human monocyte-derived macrophages inhibits HIV-1 replication by distinct mechanisms. J. Immunol. **182:**6237–6246. http://dx.doi.org/10.4049/jimmunol.0803447.
71. **Yanguez E, Garcia-Culebras A, Frau A, Llompart C, Knobeloch KP, Gutierrez-Erlandsson S, Garcia-Sastre A, Esteban M, Nieto A, Guerra S.** 2013. ISG15 regulates peritoneal macrophages functionality against viral infection. PLoS Pathog. **9:**e1003632. http://dx.doi.org/10.1371/journal.ppat.1003632.
72. **Perdiguero B, Esteban M.** 2009. The interferon system and vaccinia virus evasion mechanisms. J. Interferon Cytokine Res. **29:**581–598. http://dx.doi.org/10.1089/jir.2009.0073.
73. **Martinez FO, Gordon S, Locati M, Mantovani A.** 2006. Transcriptional profiling of the human monocyte-to-macrophage differentiation and polarization: new molecules and patterns of gene expression. J. Immunol. **177:**7303–7311. http://www.jimmunol.org/content/177/10/7303.
74. **Way KJ, Dinh H, Keene MR, White KE, Clanchy FI, Lusby P, Roiniotis J, Cook AD, Cassady AI, Curtis DJ, Hamilton JA.** 2009. The generation and properties of human macrophage populations from hemopoietic stem cells. J. Leukoc. Biol. **85:**766–778. http://dx.doi.org/10.1189/jlb.1108689.
75. **Stanley ER, Berg KL, Einstein DB, Lee PS, Pixley FJ, Wang Y, Yeung YG.** 1997. Biology and action of colony-stimulating factor-1. Mol. Reprod. Dev. **46:**4–10. http://dx.doi.org/10.1002/(SICI)1098-2795(199701)46:1<4::AID-MRD2>3.0.CO;2-V.
76. **Wiktor-Jedrzejczak W, Bartocci A, Ferrante AW, Jr, Ahmed-Ansari A, Sell KW, Pollard JW, Stanley ER.** 1990. Total absence of colony-stimulating factor 1 in the macrophage-deficient osteopetrotic (op/op) mouse. Proc. Natl. Acad. Sci. U. S. A. **87:**4828–4832. http://dx.doi.org/10.1073/pnas.87.12.4828.
77. **Mantovani A, Sica A, Sozzani S, Allavena P, Vecchi A, Locati M.** 2004. The chemokine system in diverse forms of macrophage activation and polarization. Trends Immunol. **25:**677–686. http://dx.doi.org/10.1016/j.it.2004.09.015.
78. **Mann BA, Huang JH, Li P, Chang HC, Slee RB, O'Sullivan A, Anita M, Yeh N, Klemsz MJ, Brutkiewicz RR, Blum JS, Kaplan MH.** 2008. Vaccinia virus blocks Stat1-dependent and Stat1-independent gene expression induced by type I and type II interferons. J. Interferon Cytokine Res. **28:**367–380. http://dx.doi.org/10.1089/jir.2007.0113.
79. **Mantovani A, Locati M.** 2013. Tumor-associated macrophages as a paradigm of macrophage plasticity, diversity, and polarization: lessons and open questions. Arterioscler. Thromb. Vasc. Biol. **33:**1478–1483. http://dx.doi.org/10.1161/ATVBAHA.113.300168.
80. **Klages K, Mayer CT, Lahl K, Loddenkemper C, Teng MW, Ngiow SF, Smyth MJ, Hamann A, Huehn J, Sparwasser T.** 2010. Selective depletion of Foxp3+ regulatory T cells improves effective therapeutic vaccination against established melanoma. Cancer Res. **70:**7788–7799. http://dx.doi.org/10.1158/0008-5472.CAN-10-1736.
81. **Teng MW, Ngiow SF, von Scheidt B, McLaughlin N, Sparwasser T, Smyth MJ.** 2010. Conditional regulatory T-cell depletion releases adaptive immunity preventing carcinogenesis and suppressing established tumor growth. Cancer Res. **70:**7800–7809. http://dx.doi.org/10.1158/0008-5472.CAN-10-1681.
82. **Teng MW, Swann JB, von Scheidt B, Sharkey J, Zerafa N, McLaughlin N, Yamaguchi T, Sakaguchi S, Darcy PK, Smyth MJ.** 2010. Multiple antitumor mechanisms downstream of prophylactic regulatory T-cell depletion. Cancer Res. **70:**2665–2674. http://dx.doi.org/10.1158/0008-5472.CAN-09-1574.
83. **Kirn DH, Wang Y, Liang W, Contag CH, Thorne SH.** 2008. Enhancing poxvirus oncolytic effects through increased spread and immune evasion. Cancer Res. **68:**2071–2075. http://dx.doi.org/10.1158/0008-5472.CAN-07-6515.
84. **Blasco R, Moss B.** 1992. Role of cell-associated enveloped vaccinia virus in cell-to-cell spread. J. Virol. **66:**4170–4179.
85. **Payne LG.** 1979. Identification of the vaccinia hemagglutinin polypeptide from a cell system yielding large amounts of extracellular enveloped virus. J. Virol. **31:**147–155.
86. **Reeves PM, Smith SK, Olson VA, Thorne SH, Bornmann W, Damon IK, Kalman D.** 2011. Variola and monkeypox viruses utilize conserved mechanisms of virion motility and release that depend on abl and SRC family tyrosine kinases. J. Virol. **85:**21–31. http://dx.doi.org/10.1128/JVI.01814-10.
87. **McNulty S, Powell K, Erneux C, Kalman D.** 2011. The host phosphoinositide 5-phosphatase SHIP2 regulates dissemination of vaccinia virus. J. Virol. **85:**7402–7410. http://dx.doi.org/10.1128/JVI.02391-10.